**Determination of dendritic spine morphology by the striatin scaffold protein STRN4 through interaction with the phosphatase PP2A**

Lianfeng Lin, Louisa Hoi-Ying Lo, Quanwei Lyu, and Kwok-On Lai

Supplementary Information

Additional analyses of dendritic spine morphology were performed using different cut-off ratios of head diameter to neck diameter (H/N) and length to neck diameter (L/N) for defining mushroom spines and thin spines (see Fig. S1, S3, S4 and S5). Example of images acquired by confocal microscopy and Super-resolution Structured Illumination Microscopy (SR-SIM) to illustrate the higher resolution of SR-SIM to resolve the fine structure of dendritic spine (see Fig. S2).
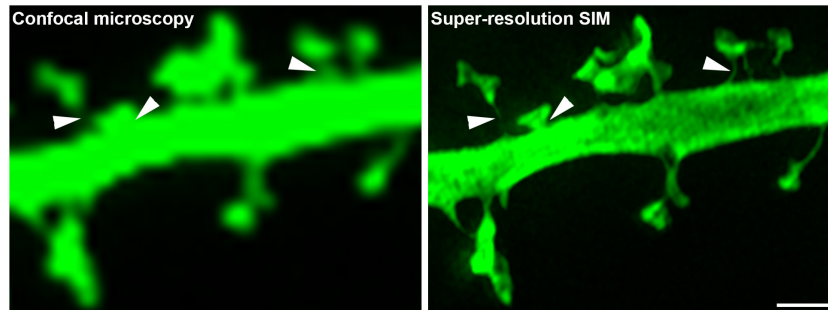
Figure S1

A

B
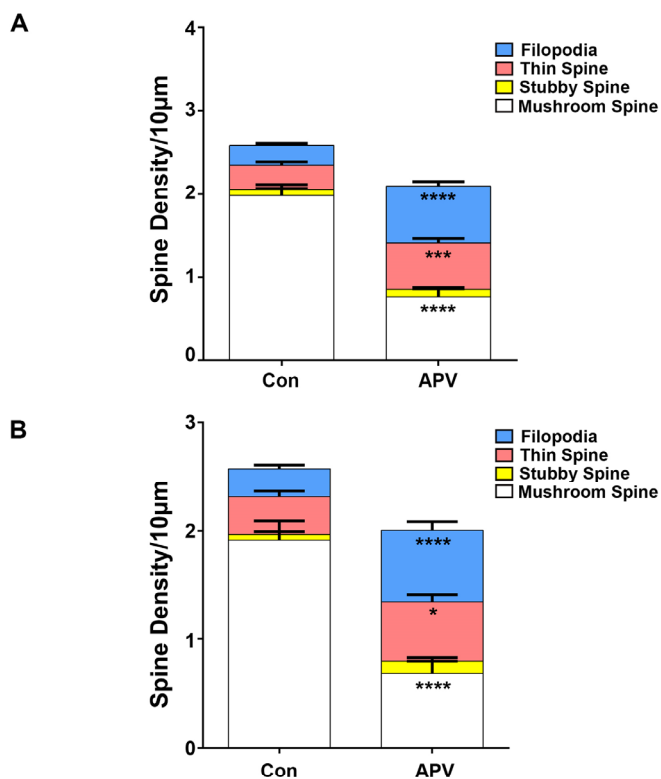
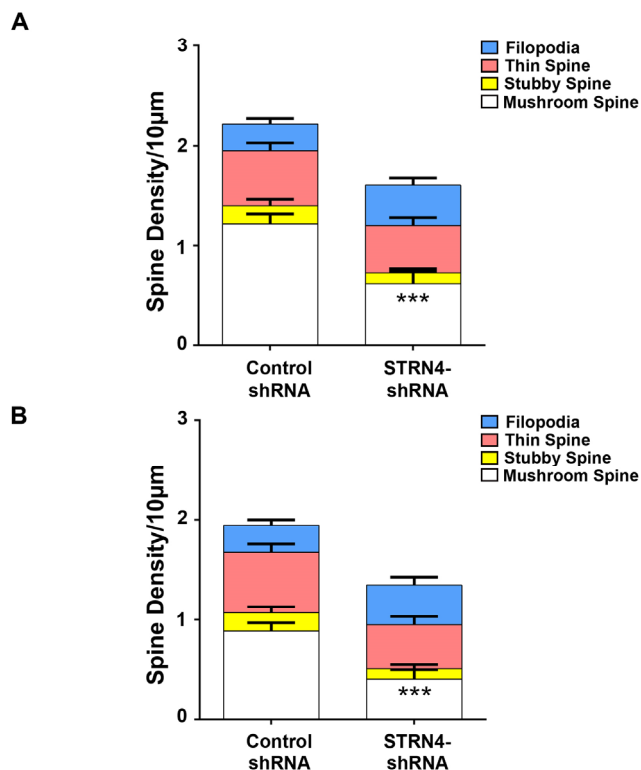**Figure S1. Effect of APV on spine morphology**

Data from Fig 3*A* were analyzed using different head diameter to neck diameter (H/N) ratio and length to neck diameter (L/N) ratio. *A*, Mushroom spine was defined as the ratio of H/N ≥ 1.7; thin spine had the ratio of $1 \leq$ H/N <1.7 and $1.7 \leq$ L/N ≤ 3. *B*, Mushroom spine was defined as the ratio of H/N ≥ 2; thin spine had the ratio of $1 \leq$ H/N <2 and $2 \leq$ L/N ≤ 3. Filopodia and stubby spine were defined using the same ratios as in Fig. 3*A*. Results were pooled from two experiments; 35 dendrites from 17 neurons were quantified for each condition. Data are mean ± SEM; *p<0.05; ***p<0.001; ****p<0.0001; Student's *t*-test.

Figure S2

Figure S2. Super-resolution SIM imaging reveals the structure of dendritic spines more clearly.
The same dendritic segment of a neuron expressing GFP was imaged by confocal microscopy (A) and
Super-resolution SIM (B), respectively. Spine necks that appeared indistinct in the confocal image
(arrowheads) were better visualized by SIM. Scale bar: 1 μm.

Figure S3

A

B

Figure S3. Effect of STRN4 knockdown on spine morphology

Data from Fig 5*B* were analyzed using different head diameter to neck diameter (H/N) ratio and length to neck diameter (L/N) ratio. *A*, Mushroom spine was defined as the ratio of H/N ≥1.7; thin spine had the ratio of 1≤ H/N <1.7 and 1.7≤ L/N≤ 3. *B*, Mushroom spine was defined as the ratio of H/N ≥ 2; thin spine had the ratio of 1≤ H/N <2 and 2≤ L/N≤ 3. Filopodia and stubby spine were defined using the same ratios as in main text (15-16 dendrites from 6 neurons were quantified for each condition; mean ± SEM; ***p<0.001, Student's *t*-test).
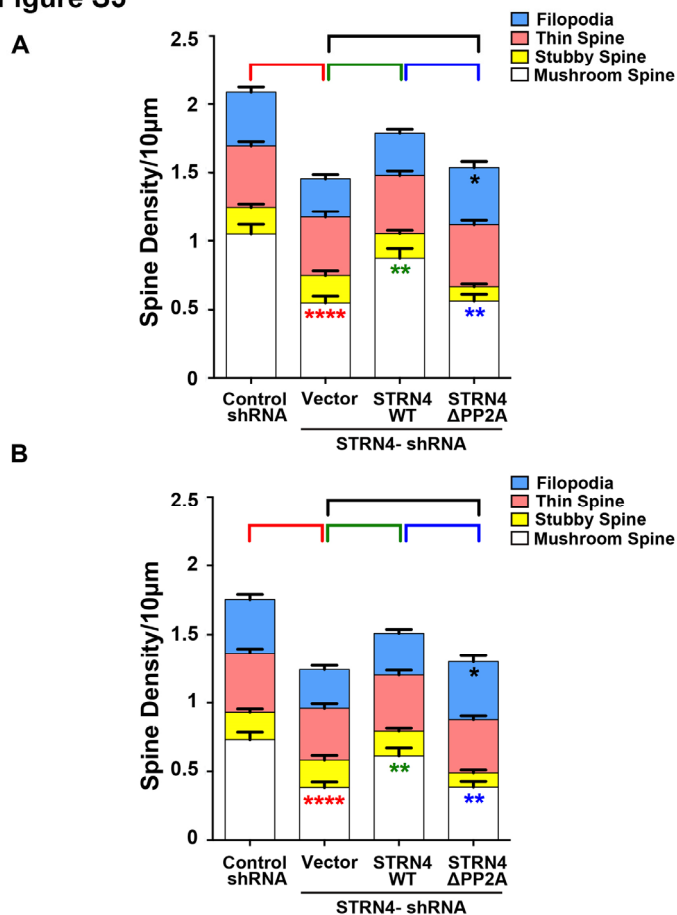
Figure S4

A

B
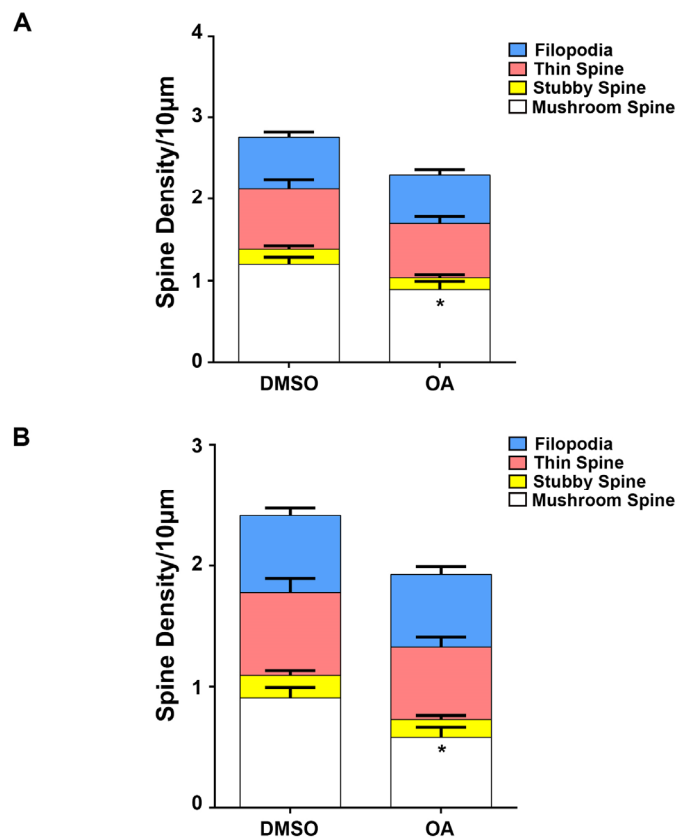
Figure S4. Effect of PP2A inhibition on spine morphology.

Data from Fig 6*B* were analyzed using different head diameter to neck diameter (H/N) ratio and length to neck diameter (L/N) ratio. *A*, Mushroom spine was defined as the ratio of H/N ≥1.7; thin spine had the ratio of 1≤ H/N <1.7 and 1.7≤ L/N≤ 3. *B*, Mushroom spine was defined as the ratio of H/N ≥ 2; thin spine had the ratio of 1≤ H/N <2 and 2≤ L/N≤ 3. Filopodia and stubby spine were defined using the same ratios as in main text. 15 dendrites from 9 neurons in each group were quantified. Data are mean ± SEM; *p<0.05, Student's *t*-test.

Figure S5. STRN4 regulates spine morphology through interaction with PP2A.

Data from Fig 7*B* were analyzed using different head diameter to neck diameter (H/N) ratio and length to neck diameter (L/N) ratio. *A*, Mushroom spine was defined as the ratio of H/N ≥1.7; thin spine had the ratio of 1≤ H/N <1.7 and 1.7≤ L/N≤ 3. *B*, Mushroom spine was defined as the ratio of H/N ≥ 2; thin spine had the ratio of 1≤ H/N <2 and 2≤ L/N≤ 3. Filopodia and stubby spine were defined using the same ratios as in main text. Results were pooled from three independent experiments (71-79 dendrites in total from 33-39 neurons in each group). Data are mean ± SEM; *p<0.05; **p<0.01; ****p<0.0001; One-way ANOVA, Tukey's multiple comparisons test.